Cancer Letters 456 (2019) 69–79

Contents lists available at ScienceDirect

Cancer Letters

journal homepage: www.elsevier.com/locate/canlet

Original Articles

IL-6 induced M1 type macrophage polarization increases radiosensitivity in HPV positive head and neck cancer

Xiaohang Chen[a,b], Enhui Fu[a], Huihuang Lou[a], Xionghui Mao[c], Bingqing Yan[a], Fangjia Tong[a], Ji Sun[c,*], Lanlan Wei[a,d,**]

[a] Department of Microbiology, Harbin Medical University, Harbin, China
[b] The Genetics Laboratory, Longgang District Maternity and Child Healthcare Hospital, Shenzhen, China
[c] Department of Otolaryngology, Head and Neck Surgery, Harbin Medical University Cancer Hospital, Harbin, China
[d] Wu Lien-Teh Institute, Harbin Medical University, Harbin, China

ARTICLE INFO

Keywords:
Human papillomavirus
HNSC
Radiotherapy
Microenvironment

ABSTRACT

Radiation is a crucial component of head and neck squamous cell carcinoma (HNSC) treatment. Human papillomavirus-positive (HPV^+) HNSC is significantly more radiosensitive than HPV^- HNSC, but the mechanism underlying this increased sensitivity is unknown. We investigated the possible involvement of macrophage subpopulations as key mediators of HNSC radiosensitivity linked to HPV status. We collected forty-one clinical HNSC specimens and determined HPV status and radiosensitivity of each sample. We investigated cytokine mediated induction of macrophage polarization by HPV^+ and HPV^- HNSC cells. Radiosensitive HNSC tissues exhibited greater numbers of infiltrating M1 macrophages than radioresistant tumor tissue samples. Moreover, M1 macrophage numbers were positively correlated with HNSC radiosensitivity. HPV^+ and HPV^- tumor cells induced macrophage polarization to M1 and M2 type, respectively. HPV^+ HNSC cells secreted more IL-6 than HPV^- cells. HPV promoted tumor cell secretion of IL-6, thereby increasing radiosensitivity through M1 polarization of macrophages. M1 macrophages represent an important tissue microenvironment factor with implications for HNSC treatment efficacy and may prove valuable as a biomarker of radiation sensitivity.

1. Introduction

Head and neck squamous cell carcinoma (HNSC) is the sixth most common cancer worldwide and the incidence of human papillomavirus (HPV) involved HNSC is increasing yearly [1,2]. Radiotherapy is a very important component of HNSC treatment and tumor radiosensitivity is significantly higher among HPV^+ patients compared to those who are HPV^- [3]. No mechanism explaining the increased radiosensitivity of HPV^+ HNSC has yet emerged from studies examining possible links to DNA damage repair, cell cycle regulation or tumor tissue hypoxia [4]. It is possible that HPV^+ HNSC radiosensitivity may be linked, at least in part, to heterogeneous populations of tumor-infiltrating immune cells [5]. Given the importance of radiation in HNSC treatment it is clear that additional studies are needed to explore underlying mechanisms in order to optimize individualized patient therapy.

Tumor-associated macrophages (TAMs) are important components of the immune microenvironment. TAMs can be further classified into M1 or M2 macrophages, which play roles in influencing levels of tumor radiosensitivity through multiple signaling pathways [6]. These TAMs can therefore be of value in guiding individualized patient treatment. M1 macrophages are reportedly linked to radiosensitivity in a variety of tumors and HPV has been shown to promote infiltration of M1 macrophages into the HNSC tissue microenvironment [7,8]. Here, we investigate whether HPV plays a key role in radiosensitization of HNSC tumor cells by regulating the polarization of macrophages towards the M1 type. These studies have the potential to increase understanding of immune regulatory network involvement in determining HPV^+ HNSC radiosensitivity and thereby guiding development and practice of improved patient treatment regimens.

2. Materials and methods

2.1. Patient information and clinical samples

Clinical samples were obtained from forty-one HNSC patients treated by the Department of Head and Neck Surgery, Harbin Medical

* Corresponding author. Department of Otolaryngology, Head and Neck Surgery, Harbin Medical University Cancer Hospital, Harbin, China.
** Corresponding author. Department of Microbiology, Wu Lien-Teh institute, Harbin Medical University, Harbin, China.
E-mail addresses: drsunji@163.com (J. Sun), weilanlan_1119@163.com (L. Wei).

https://doi.org/10.1016/j.canlet.2019.04.032
Received 28 October 2018; Received in revised form 22 April 2019; Accepted 25 April 2019

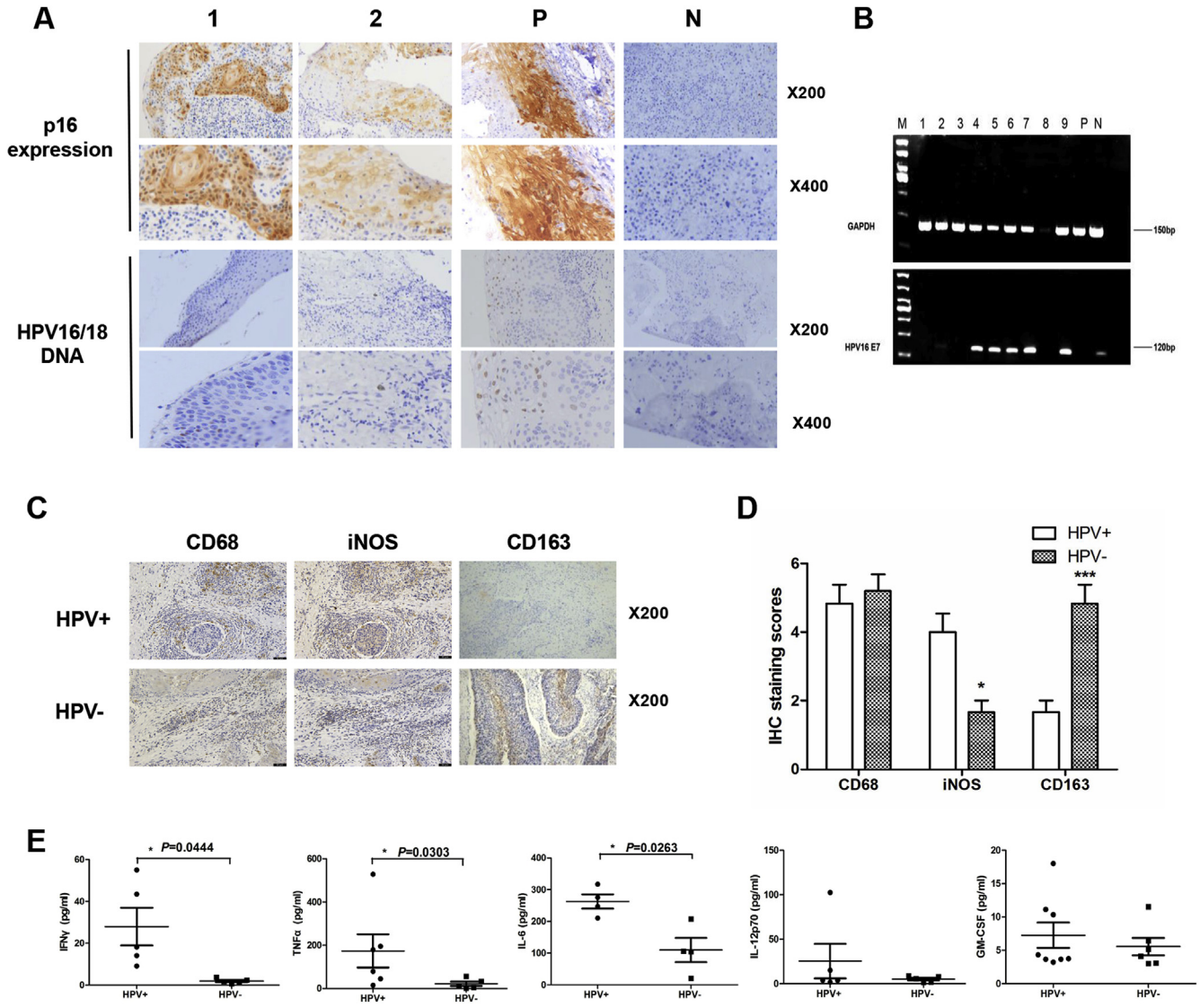

Fig. 1. Increased M1 macrophage infiltration in HPV$^+$ HNSC. (A) IHC analysis of p16 expression in HNSC. *In situ* hybridization analysis of HPV16/18 DNA in HNSC cells (1, 2 are clinical samples; P, cervical cancer positive control; N, glioma negative control) (magnification × 200 and × 400). **(B)** PCR-based detection of GAPDH (DNA integrity control) and HPV16 E7 DNA in HNSC (M, Molecular weight marker; 1–9, clinical specimens; P, cervical cancer positive control; N, glioma negative control). **(C)** IHC analysis of CD68, iNOS and CD163 expression in HNSC (magnification × 200 and × 400). **(D)** Quantitation of HNSC CD68, iNOS and CD163 IHC data. **(E)** Multi-cytokine assay results. Quantitative analysis based on triplicate experiments. Data presented as mean ± SEM. $^*P < 0.05$,$^{**}P < 0.01$.

University Cancer Hospital between June 2016 and December 2017. The study was approved by the Ethics Review Committee of Harbin Medical University (HMUIRB20180008). All patients provided written informed consent. HNSC tumor samples (confirmed diagnosis, grades I to IV) were obtained along with control adjacent tissues (2 cm from edge of tumor). Tumor and control normal tissue samples were confirmed by pathological examination. Tissue samples were paraffin embedded and rapidly frozen in liquid nitrogen for subsequent analysis. And all the samples obtained from the patients who not treated with radiation or chemotherapy before surgery.

2.2. Cells lines

HPV16$^+$ HNSC cell lines SCC47 and SCC104 and HPV$^-$ cell lines CAL33 and SAS were kindly provided by Dr. Henning Willers (Harvard University, Boston, USA). HPV$^+$ HNSC cell line SCC90 was purchased from the Chinese Academy of Sciences Cell Bank (Shanghai, China). The cell line CAL27 was a kind gift of Professor Songbin Fu (Harbin Medical University, Harbin, China). The monocyte cell line THP1 is maintained in our laboratory. HNSC cells were cultured in DMEM (HyClone, USA) containing 10% fetal bovine serum (FBS, Biological Industries, USA), penicillin (100 U/ml, Gibco, USA) and streptomycin (100 mg/ml, Gibco, USA). THP1 cells were cultured in RPMI-1640 medium (HyClone, USA) containing 10% FBS. For cytokine analysis conditioned medium was collected after 48 h of culture or when cells achieved 80% confluence.

2.3. Plasmids

Plasmid pc-HPV16 was kindly provided by Dr. Michelle Ozbun (University of New Mexico School of Medicine, USA). Plasmid pcDNA-HPV16E5/E6/E7 was obtained from Kangcheng (Shanghai, China).

2.4. Macrophage polarization and neutralization studies

THP1 cell macrophage differentiation was induced by phorbol treatment with 12-myristate 13-acetate (PMA) for 24 h. This was followed by addition of 100 ng/ml LPS and 20 ng/ml IFNγ (for M1

Table 1
Patient demographic and clinical characteristics.

Character	HPV+ (N = 16)	HPV- (N = 25)	*P*
Gender, n (%)			0.35
Male	13 (43.3)	17 (56.67)	
Female	3 (27.3)	8 (72.7)	
Age (years)			
Mean	58.9	58	
Range	38-77	45-73	
Anatomic site, n (%)			0.32
Larynx	12 (44.4)	15 (55.6)	
Oropharynx	4 (28.6)	10 (71.4)	
Tobacco smoking, n (%)			0.46
Yes	12 (42.9)	16 (57.1)	
Never	4 (30.8)	9 (69.2)	
Alcohol use, n (%)			0.72
Yes	6 (42.9)	8 (57.1)	
Never	10 (37.0)	17 (63.0)	
T stage, n (%)			0.83
T1-T2	15 (39.5)	23 (60.5)	
T3-T4	1 (33.3)	2 (66.7)	
N stage, n (%)			0.46
N0	12 (42.9)	16 (57.1)	
N1-N3	4 (30.8)	9 (69.2)	
M stage, n (%)			
M0	16 (39.0)	25 (61.0)	
M1	0	0	
Differentiation, n (%)			0.07
Poor	1 (20.0)	4 (80.0)	
Moderate	5 (25.0)	15 (75.0)	
Well	9 (60.0)	6 (40.0)	

macrophages) or 20 ng/ml IL-4 and 20 ng/ml IL-13 (for M2 macrophages), or 20 ng/ml IL-6 for 48 h. For co-culture and neutralization experiments, HNSC cell lines were seeded on THP1 cells separated by 0.4 μm-pore transwells. Neutralizing anti-IL-6 (ab6672, Abcam) was added daily to a concentration of 2.5 μg/ml for 3 days.

2.5. Immunohistochemistry

Immunohistochemical (IHC) staining was performed as previously described [9]. Rabbit anti-p16 antibody was purchased from Zhongshan Goldenbridge (China). P16 was considered overexpressed if immunostaining appeared strong and diffuse with > 60% of tumor cells $p16^+$. Rabbit anti-iNOS and anti-CD163 antibodies were purchased from Abcam (UK). Rabbit anti-CD68, anti-TNFα antibody was purchased from Proteintech Group (USA). Briefly, endogenous peroxidase was blocked with 3% hydrogen dioxide for 30 min. Antigens in the sections were retrieved by autoclaving in citrate repair buffer for 2 min. Sections were washed with phosphate-buffered saline (PBS) three times to minimize non-specific background, then incuted with antibody at 4°Covernight, followed by incubation with Two-Step IHC reagents and 3,3-diaminobenzidine substrate (Zhongshan Goldenbridge, China). Finally, the sections were counterstained with hematoxylin. Staining of IHC was assessed in a series of randomly selected ten high-power fields. The stained slides were reviewed and scored independently by two observers blinded to the patients' information. The scores were determined by combination of the proportion of positively stained cells and the intensity of staining as follows: 0 (no positive cells), 1 (< 10% positive cells), 2 (10–50% positive cells), and 3 (> 50% positive cells). Staining intensity was classified according to the following criteria: 0 (no staining), 1 (weak staining = light yellow), 2 (moderate staining = yellow brown), and 3 (strong staining = brown). Staining index was calculated as the staining intensity score × the proportion score. Using this method, the expression of IHC was evaluated by determining the staining index, with scores 0, 1, 2, 3, 4, 6, or 9.

2.6. Detection of HPV in clinical specimens

Tissue samples were processed as previously described. DNA was extracted and sample integrity was confirmed by PCR using GAPDH gene-specific primers. HPV status was determined using a highly sensitive PCR protocol and HPV16 E7 degenerate primers. PCR products were separated by electrophoresis on 1.5% agarose gels and visualized by GCLSTAIN staining. HPV genotyping was performed according to the manufacturer's instructions of HPV genotyping kit for 23 types (Yaneng, China).

2.7. In situ hybridization

HPV16/18 DNA sequences were detected by *in situ* hybridization using the DNA-ISH Kit (Kaipu, China) according to manufacturer's instructions.

2.8. Immunofluorescence-based radiosensitivity assay

Frozen tissue sections were fixed in 10% neutral formaldehyde for 15 min, permeabilized with 0.5% Triton X-100 and then blocked for 30 min with 5% BSA. Sections were incubated overnight at 4 °C with mouse anti-γH2AX (Ser139) (Merck-Millipore, Germany). Following three washes with PBS the sections were incubated with secondary antibody, washed three times and then mountedin antifade mounting medium containing DAPI (Solarbio, China).

2.9. Multi-cytokine assay

Conditioned medium (CM) was aliquoted within 1 h of collection and stored frozen (−80 °C) for subsequent analysis. Six cytokines were analyzed using immunoassay kits from Biolegend (for IL-6, IL-10, IL-12p70 and IFNγ) and R&D Systems (TNFα and GM-CSF).

2.10. Irradiation

The standard procedures were listed in previously literature [10,11]. All the specimens were collected in tubes with saline and bring into incubator at 37 °C within 1 h (or so) of surgery. Then the tissues were cut with a scalpel into pieces of 3–5 mm: one for untreated control, one for irradiated. The tissues were cultured in 10% RPMI-1640 medium, and immediately received irradiation in our lab. The optimal dose of X-ray irradiation was 6 Gy (RadSource RS2000, US). Then the specimens were cultured at 37 °C, humidified incubator for 24 h. After 24 h, the tissues were rinsed with fresh PBS and rapidly frozen in Optimal Cutting Temperature (OCT) compound (SAKURA, Japan) with liquid nitrogen. The tissues need to be cut with a frozen microtome while embedded in OCT. Then the tissue slices need to be placed on glass slides and stored at −80 °C in sealed slide boxes. Thickness of tissue slices should be 3–5 μm.

2.11. Statistical analysis

Analysis was performed using SPSS (SPSS Inc., IL) and GraphPad Prism 5 (GraphPad Software Inc., CA) software. Statistical analyses comparing two groups were carried out using the nonparametric Mann-Whitney test. More than two groups were assessed by analysis of variance (ANOVA) for multiple pairs of interest without *a priori* selection. All statistical tests were two-sided. Differences were considered statistically significant at P values < 0.05. Experiments were performed at least three times. Values are presented as mean ± SD unless otherwise noted.

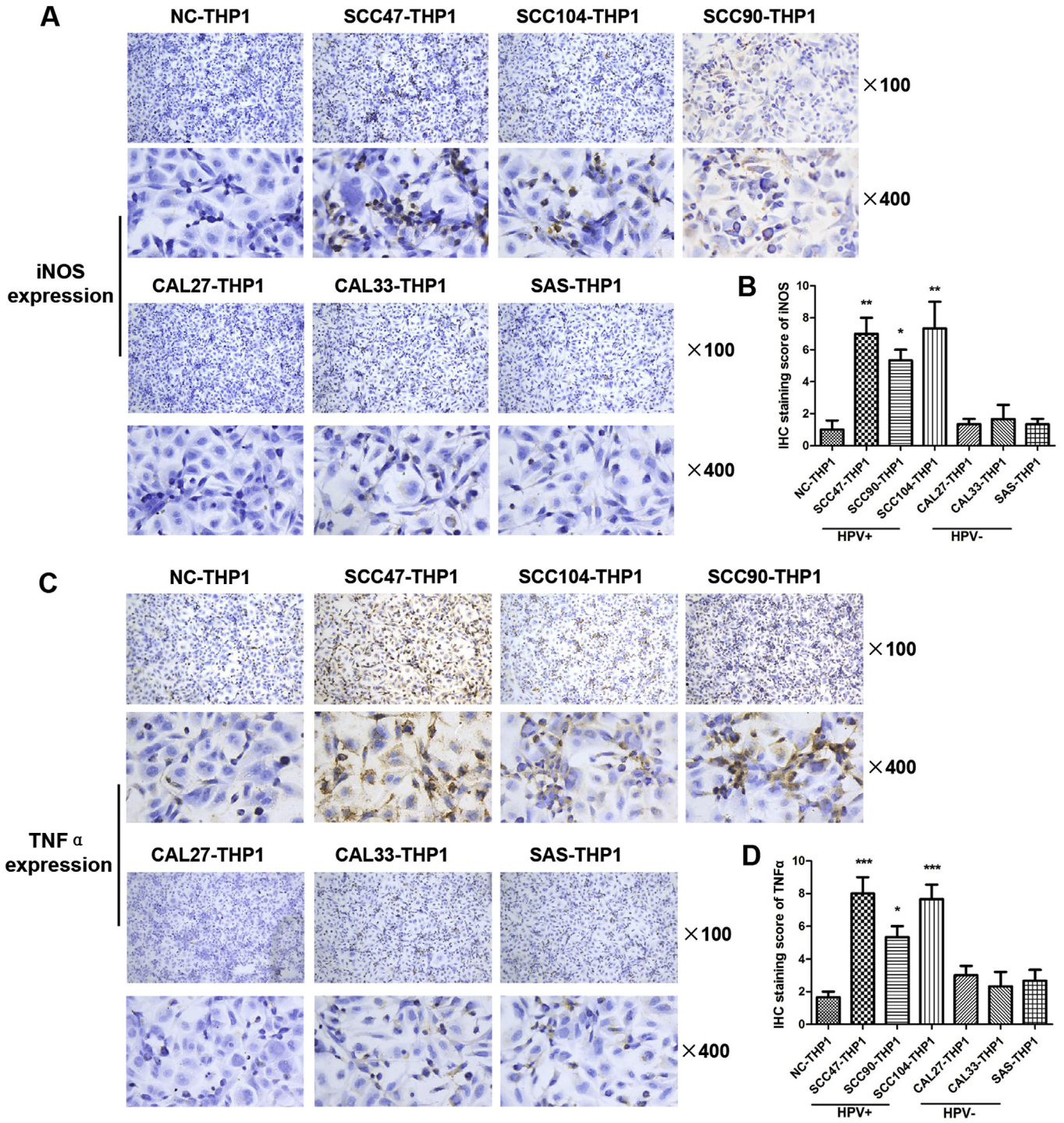

Fig. 2. Macrophage polarization to M1 type by HPV$^+$ HNSC culture supernatant. (A) IHC analysis of iNOS expression in HNSC culture supernatant-treated THP1 macrophages (NC, normal control culture; SCC47/SCC104/SCC90, HPV$^+$ HNSC cell line culture supernatant; CAL27/CAL33/SAS, HPV$^-$ HNSC cell line culture supernatant) (magnification × 100 and × 400). **(B)** Quantitation of IHC iNOS expression data. **(C)** IHC analysis of TNFα expression in HNSC culture supernatant-treated THP1 macrophages(magnification × 100 and × 400). **(D)** Quantitation of IHC TNFα expression data. **(E)** IHC analysis of CD163 expression in HNSC culture supernatant-treated THP1 macrophages (magnification × 100 and × 400). **(F)** Quantitation of IHC CD163 expression data. **(G–K)** Multi-cytokine assay results. Quantitative analysis based on triplicate experiments. Data presented as mean ± SEM. $^*P < 0.05$,$^{**}P < 0.01$, $^{***}P < 0.001$.

3. Results

3.1. Increased M1 macrophage infiltration in HPV$^+$ HNSC

Forty-one clinical specimens were collected from HNSC patients ranging in age from 38 to 77 years (mean 58.5 yr, SD 7.9 yr). HPV status was determined using a variety of approaches including IHC detection of p16 and HPV16/18 DNA detection by *in situ* hybridization (Fig. 1A) and PCR analysis of extracted DNA. HPV was detected by PCR in 16/41 (41.5%) patient samples. HPV16 was the most common HPV type, detected in 14/41 (34.1%) cases (Fig. 1B). Specimens were divided into HPV$^+$ (N = 16) and HPV$^-$ (N = 25) experimental groups. Patient information is summarized in Table 1. The prevalence of HPV$^+$ HNSC in Heilongjiang Province was approximately 39.0%. Most HNSC patients

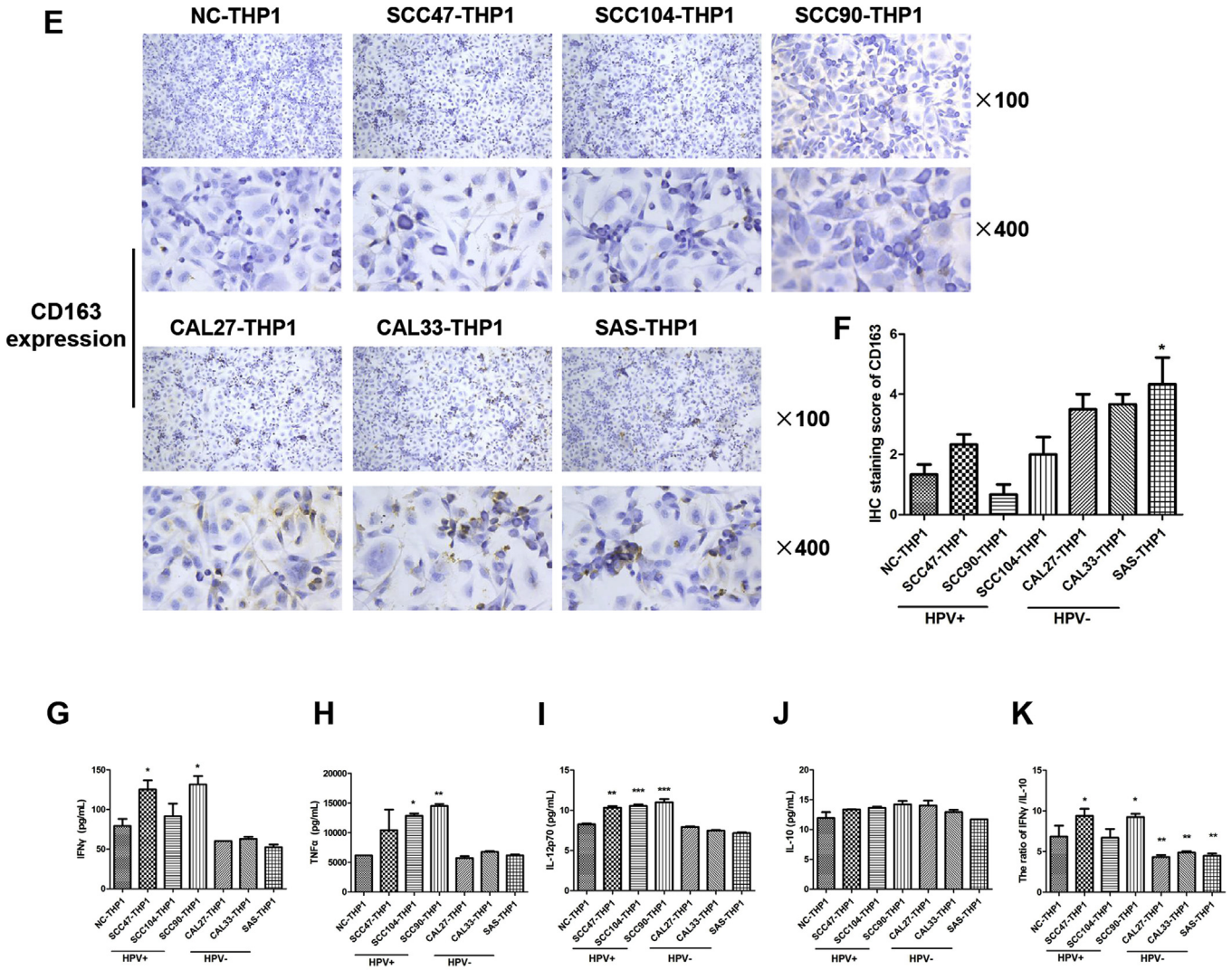

Fig. 2. (*continued*)

were male with a history of tobacco and alcohol use. Our findings suggest that HPV may influence the differentiation of HNSC to some extent.

IHC was used to comparatively analyze expression of macrophage subpopulation markers inducible nitric oxide synthase (iNOS, specific for M1 macrophages) and CD163 (M2 macrophages) in HPV^+ and HPV^- clinical specimens (Fig. 1C). M1 macrophages were significantly more prevalent in HPV^+ HNSC, while M2 macrophages were less abundant in HPV^+ HNSC compared to HPV^- HNSC, $P < 0.05$ (Fig. 1D).

To examine differential expression of macrophage-associated cytokines in HPV^+ and HPV^- clinical specimens, total protein was extracted and analyzed using a multi-cytokine assay (Fig. 1E–K). M1 macrophage signature cytokines including IFNγ, TNFα and IL-6 were more abundantly expressed in HPV^+ than HPV^- HNSC ($P < 0.05$). Although not statistically significant, M1 macrophage cytokine markers IL-12p70 and GM-CSF also appeared higher in HPV^+ HNSC. Expression levels of IL-10 in clinical specimens were very low (< 1 pg/mL) and could not be analyzed.

3.2. M1 macrophage polarization by HPV^+ HNSC conditioned medium

To further investigate the influence of HPV on macrophage differentiation, we exposed THP1 cells for 48 h to 20% CM prepared from cultures of HPV^+ HNSC cell lines SCC47, SCC90 and SCC104 and HPV^- HNSC cell lines CAL27, CAL33 and SAS. Macrophage polarization was then assessed (Fig. 2A–F). HPV^+ HNSC CM increased THP1 cell expression of M1 markers iNOS and TNFα whereas HPV^- HNSC CM increased expression of M2 marker CD163. HPV + HNSC CM induction of CD163 expression in THP1 cells was inconsistent: SCC90 CM decreased CD163 levels while SCC47 and SCC104 CM somewhat increased CD163.

A multi-cytokine assay was used to compare cytokine levels in THP1 cell culture supernatants (Fig. 2G–K). Secreted IFNγ, TNFα and IL-12p70 levels were significantly higher in supernatants of THP1 cells cultured with HPV^+ HNSC CM compared to HPV^- HNSC CM. Secreted IL-10 levels were similar in supernatants of THP1 cells cultured with either HPV^+ or HPV^- HNSC CM. A comprehensive analysis of M1 and M2 related cytokine ratios suggested that HPV^+ HNSC CM induced THP1 macrophage polarization to the M1 type, while HPV^- HNSC CM induced M2 polarization.

3.3. M1 macrophage polarization by HPV^+ HNSC cell co-culture

We further investigated HPV linked macrophage polarization in the context of HNSC by co-culturing THP1 and HPV^+ or HPV^- HNSC cells. After 48 h of co-culture, HPV^+ HNSC cells induced significantly higher expression of iNOS and TNFα in THP1 cells compared to co-culture with HPV^- HNSC cells. By contrast, HPV^- HNSC co-culture induced significantly increased expression of CD163 in THP1 cells (Fig. 3A–F). Using a multi-cytokine assay we observed increased secretion of IFNγ,

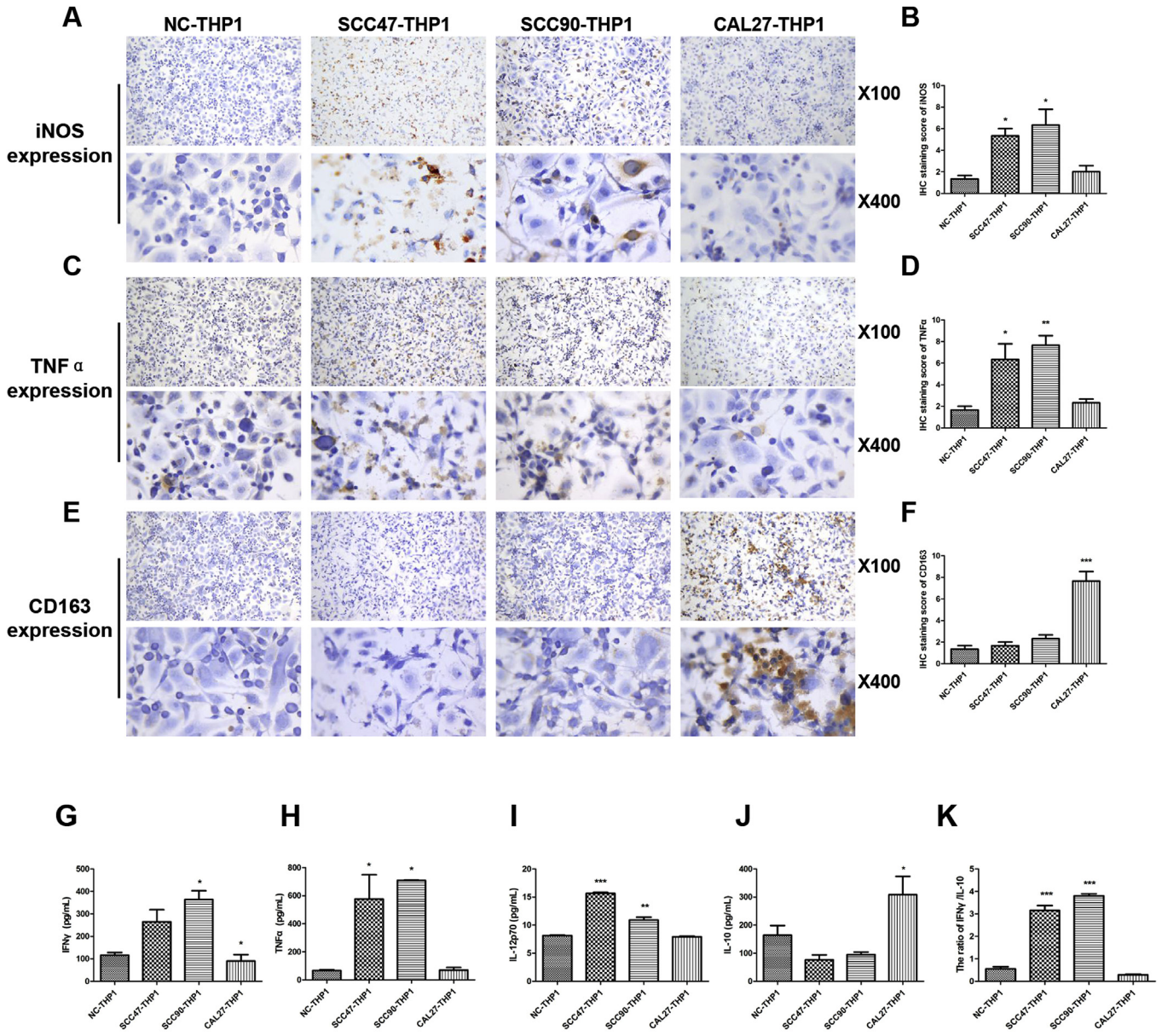

Fig. 3. THP1 cell M1 polarization by HPV$^+$ HNSC co-culture. (A) IHC analysis of iNOS expression in THP1 macrophages co-cultured with HNSC cells (NC, normal control culture; SCC47/SCC104/SCC90, HPV$^+$ HNSC cell lines) (magnification × 100 and × 400). **(B)** Quantitation of IHC iNOS expression data. **(C)** IHC analysis of TNFα expression in THP1 macrophages co-cultured with HNSC cells. **(D)** Quantitation of IHC TNFα expression data. **(E)** IHC analysis of CD163 expression in THP1 macrophages co-cultured with HNSC cells. **(F)** Quantitation of IHC CD163 expression data. **(G–K)** Multi-cytokine assay results. Quantitative analysis based on triplicate experiments. Data presented as mean ± SEM.*$P < 0.05$,**$P < 0.01$, ***$P < 0.001$.

TNFα and IL-12p70 and decreased IL-10 secretion by THP1 cells after co-culture with HPV + HNSC cells (Fig. 3G–K). Comprehensive analysis of M1 and M2 related cytokine ratios again suggested that HPV$^+$ HNSC cell co-culture induced THP1 macrophage polarization to the M1 type, while HPV$^-$ HNSC co-culture induced M2 polarization.

3.4. M1 macrophage prevalence positively correlated with HNSC radiosensitivity

HPV$^+$ and HPV$^-$ HNSC tissue samples were treated with 6 Gy of X-ray radiation. Within 24 h of irradiation we assessed γ-H2AX foci by immunofluorescence (IF) (Fig. 4A–B). Quantitative IF analysis showed that control nonirradiated HPV$^+$ and HPV$^-$ samples had similar γ-H2AX foci (mean values of 12.20% and 10.25%, respectively). Radiation treatment increased overall values of γ-H2AX foci to 48.07% for HPV$^+$ HNSC samples, significantly higher than the 22.79% observed for HPV$^-$ HNSC samples. These studies indicated that the HPV$^+$ HNSC tumors examined in this study were significantly more radiosensitive than the HPV$^-$ HNSC tumors, as expected from previously published research. We used a Spearman model to look for a correlation between M1 macrophage subtype prevalence based on IHC examination of markers and radiosensitivity of HNSC based on γ-H2AX foci (Fig. 4C). The results of this analysis indicated a significant positive correlation between iNOS$^+$ macrophages and radiosensitivity.

3.5. HPV status correlated with HNSC cytokine secretion

Our results suggested that HPV might influence THP1 polarization to an M1 macrophage subtype through the action of cytokines. A multi-cytokine assay was used to analyze secreted polarization-associated cytokines in HPV$^+$ and HPV$^-$ HNSC cell culture supernatants (Fig. 5A–D). We found IL-6 levels to be much higher in the supernatants

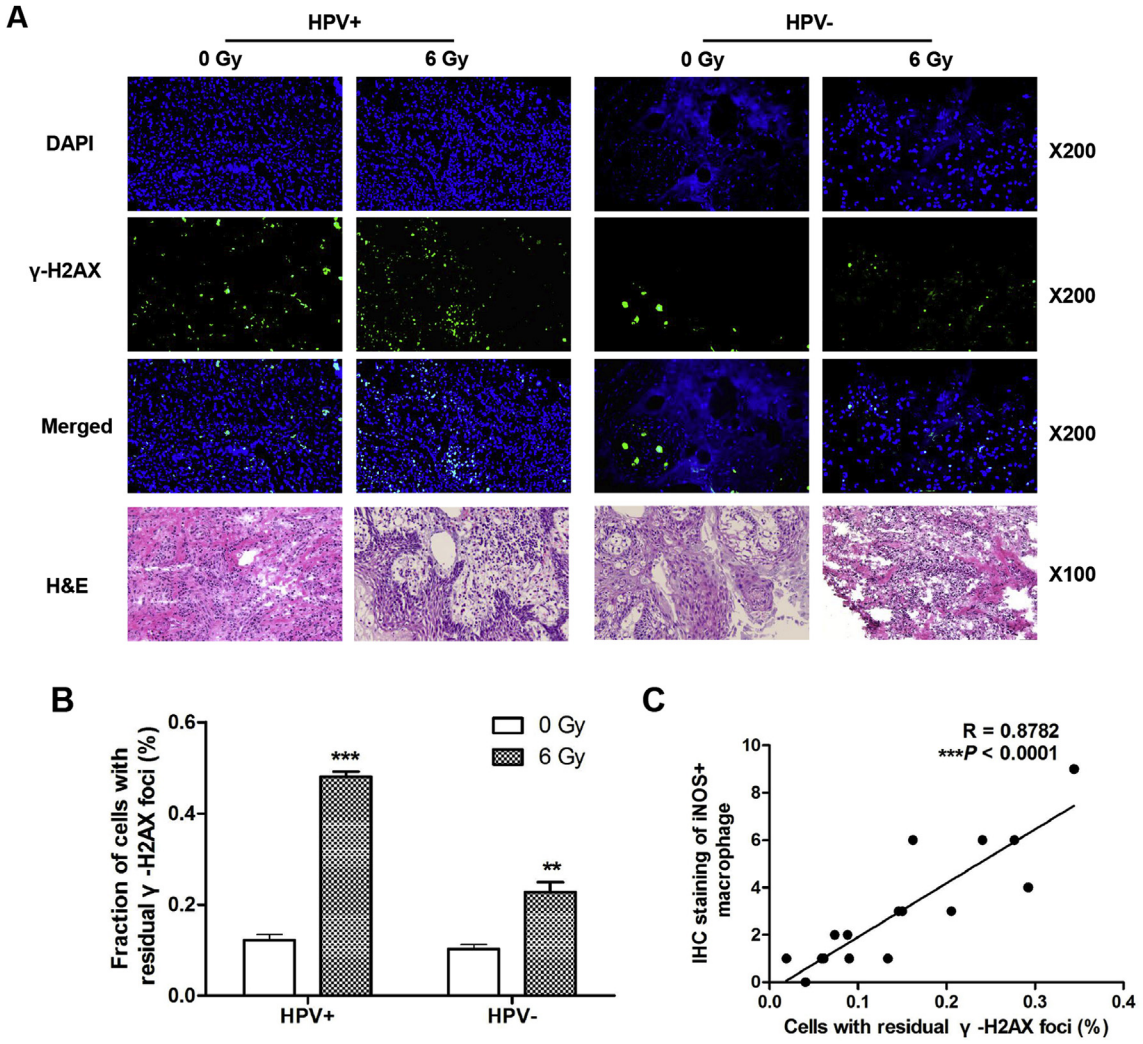

Fig. 4. Positive correlation of HNSC radiosensitivity with M1 macrophage prevalence. (A) Immunofluorescence detection of γ-H2AX foci 24 h after irradiation and corresponding H&E staining for tumor cell identification (magnification × 100 and × 200). **(B)** Quantitation of γ-H2AX foci 24 h after irradiation. **(C)** Correlation of γ-H2AX foci and iNOS$^+$ (M1) macrophage prevalence (determined by IHC). Quantitative analysis based on triplicate experiments. Data presented as mean ± SEM. $^{**}P < 0.01$,$^{***}P < 0.001$.

of HPV$^+$ cells (particularly SCC90 cells) compared to HPV$^-$ cells. We also observed slightly increased IFNγ in HPV$^+$ HNSC supernatants but at levels below that required to elicit polarization effects, indicating that HNSC cells may not be the main source of IFNγ in the tumor microenvironment. In addition, TNFα and GM-CSF levels were similar in supernatants of HPV$^+$ and HPV$^-$ cells, suggesting that expression of these cytokines is not correlated with HPV status.

We investigated whether HPV16 overexpression could induce secretion of IL-6 by the HPV$^-$ HNSC cell line CAL27 (Fig. 5E). CAL27 cells transfected with the pc-HPV16 construct were shown to express HPV16 mRNA within 48 h of transfection, with increased IL-6 protein levels. IL-6 secretion reached a maximum at 24 h after transfection and was still highly expressed at 48 h.

To further examined HPV16 oncogene involvement in IL-6 secretion by HNSC cells by generating CAL27 cells overexpressing HPV16 E5/E6/E7 (Fig. 5F). We found that HPV16 E5 and E7 slightly increased IL-6 secretion while E6 led to a decrease. Therefore, we showed that HPV16 induced secretion of IL-6 but specific functions of HPV16 oncogenes remain undefined.

3.6. IL-6-induced M1 macrophage polarization increased radiosensitivity of HNSC

We tested the effect of IL-6 on macrophage differentiation. THP1 cells treated with PMA served as a negative control. M1 and M2 polarized macrophages induced by treatment of THP1 cells with LPS plus IFNγ and IL-4 plus IL-13 cytokines, respectively, served as positive controls (Fig. 6A–F). IL-4 and IFNγ are known to play opposing roles in macrophage differentiation. We observed that IL-4 plus IL-13 induced expression of CD163 and IL-10, whereas LPS plus IFNγ induced expression of iNOS. A multi-cytokine assay showed that LPS plus IFNγ induced secretion of TNFα and IL-12p70, while IL-4 plus IL-13 induced secretion of IL-10. IL-6 significantly up-regulated expression of TNFα and downregulated expression of CD163 in THP1 cells (Fig. 6A–F). IL-6 significantly increased secretion of TNFα and IL-12p70, while decreasing secretion of IL-10 (Fig. 6G–K). IFNγ secretion was similar for IL-6 treated THP1 cells and M1 and M2 macrophages. However, IL-6 treatment of macrophages led to a significant increase in IFNγ/IL-10 ratio. These experiments indicated that IL-6 promoted macrophage polarization to an M1 type.

Next the influence of M1 macrophage polarization on radiosensitivity was detected. IL-6-induced THP1 cells were co-cultured with tumor cells CAL27. Then the radiosensitivity of CAL27 cells was

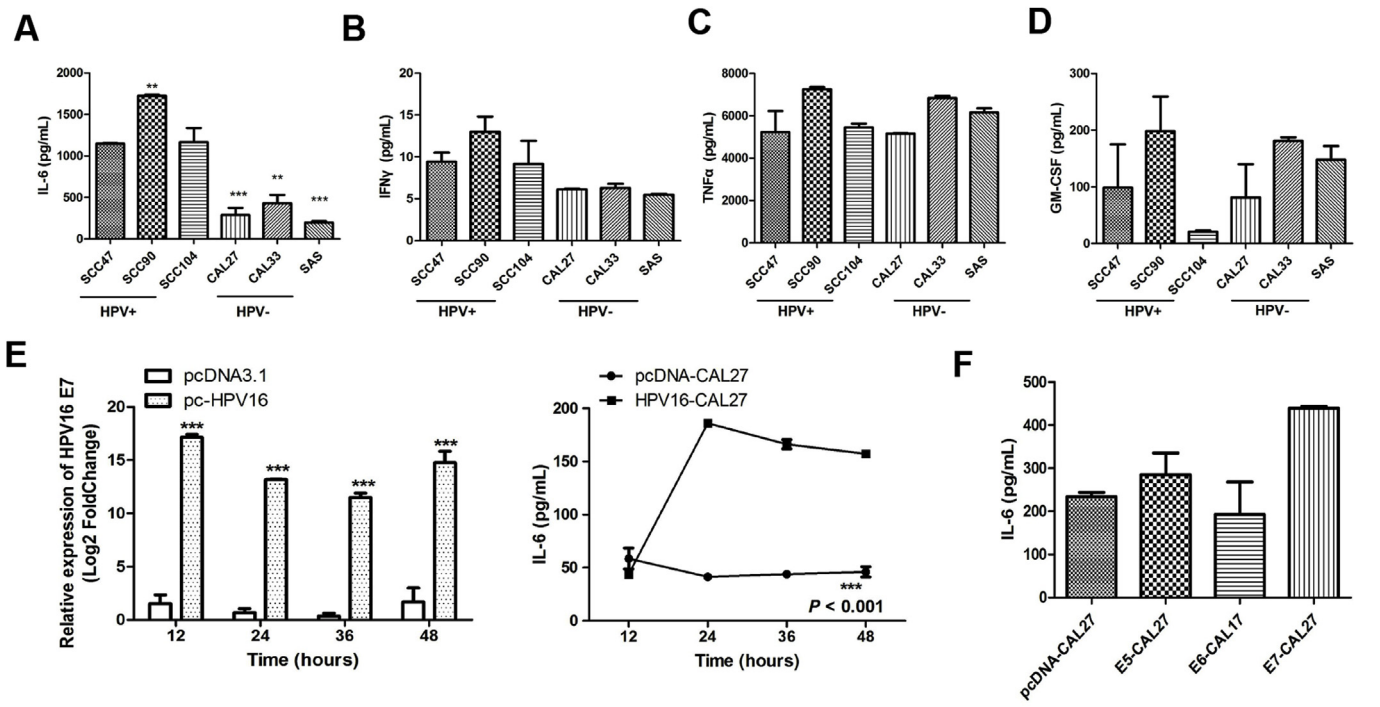

Fig. 5. Increased IL-6 secretion induced by HPV. (A) Analysis of IL-6 in HNSC culture supernatant (SCC47/SCC104/SCC90, HPV$^+$ HNSC cell line culture supernatant; CAL27/CAL33/SAS,HPV$^-$ HNSC cell line culture supernatant) **(B)** Analysis of IFNγ in HNSC culture supernatant. **(C)** Analysis of TNFα in HNSC culture supernatant. **(D)** Analysis of in GM-CSF HNSC culture supernatant. **(E)** q-RT PCR analysis of HPV16 E7 expression in CAL27 cells transfected with HPV16 construct. Analysis of IL-6 expression in HPV16 transfected CAL27 cell culture supernatant. **(F)** Analysis of IL-6 expression in pc-E5/E6/E7 transfected CAL27 cell culture supernatant at 36 h. Quantitative analysis based on triplicate experiments. Data presented as mean ± SEM. $^{**}P < 0.01$, $^{***}P < 0.001$.

detected. IL-6-induced THP1 cells increased the radiosensitivity of CAL27 compared with control (Fig. 6L). It suggested that IL-6-induced M1 macrophage increased radiosensitivity of HNSC.

3.7. IL-6 required for HPV associated M1 macrophage polarization

To investigate IL-6 involvement in M1 polarization linked to HPV we established an HPV$^+$ HNSC and THP1 cell co-culture system to test the effects of an IL6 neutralizing antibody (Fig. 7A–F). IHC analysis showed that relative to control, the addition of anti-IL6 significantly inhibited TNFα and increased CD163 expression by THP1 cells. iNOS expression also appeared to be inhibited, though not to a statistically significant level. Multi-cytokine assays revealed that TNFα secretion was significantly inhibited by anti-IL-6 (Fig. 7G–K). IL-6 neutralizing antibody had no detectable effect on secretion of IL-12p70 or IL-10. We also found that the SCC90 cell line-induced secreted IFNγ/IL10 ratio was significantly decreased by anti-IL6, while no significant effect was detected in the case of SCC47 cell co-culture. M1 macrophage polarization associated with HPV$^+$ HNSC, therefore, was inhibited by IL-6 neutralizing antibody.

4. Discussion

HPV has come to be regarded as an important pathogenic factor that influences HNSC radiosensitivity. While it is known that HPV$^+$ HNSC is more radiosensitive than HPV$^-$ HNSC, the mechanism underlying this important distinction remains unclear. Radiotherapy exerts a non-target, qualitative effect on tumors by inducing intracellular genetic damage and bystander cell killing. M1 macrophages are the main source of bystander damage and in radiotherapy-sensitive mice most macrophages are of the M1 type, while M2 macrophages predominate in radiotherapy-insensitive mice that exhibit an inhibited inflammation phenotype. We previously reported results based on bioinformatics indicating that M1 macrophage tissue infiltration was enhanced in HPV$^+$ compared to HPV$^-$ HNSC. This led us to explore a possible correlation between M1 macrophage prevalence and radiosensitivity in HNSC. Our studies indeed confirm that M1 macrophages in HNSC tissues are positively correlated with radiotherapy sensitivity.

Despite numerous studies confirming that TAM subtypes are important considerations for tumor prognosis and treatment, no uniform standard methods have been established for macrophage activation or typing either *in vitro* or *in vivo*. In the current study we used classical markers for M1 and M2 macrophages to examine HNSC associated TAMs. Distinguishing M1/M2 macrophage requires assessments of cell surface markers, ROS/RON products and secreted cytokine levels [12]. Compared to M2 macrophages, M1 macrophages exhibit increased expression of iNOS and inflammatory cytokines TNFα, IFNγ, IL-1B, IL-12A, IL-12B and IL-23A, while IL-10 expression is down-regulated [13–15].

Few prior studies have examined effects of HPV status on M1/M2 macrophage typing. We observed more infiltrating M1 macrophages in HPV$^+$ compared to HPV$^-$ HNSC. We also demonstrated that HPV$^+$ HNSC cell culture supernatant promoted macrophage polarization towards an M1 subtype while HPV$^-$ HNSC culture supernatant induced M2 macrophage polarization. These observations are consistent with the published literature [16]. HPV $^+$ SCC47 and SCC90 cell culture supernatants were both somewhat more effective than SCC104 culture supernatants in promoting M1 polarization. SCC47 and SCC90 cells harbor multiple copies of the HPV genome, while SCC104 cells have only a single copy. The M1 polarization potential of HPV$^+$ HNSC cell supernatants may therefore be related to levels of HPV gene expression.

HPV could affect the expression profiles of secretory factors that regulate the immune microenvironment. It is known that following opportunistic HPV infection, increased mucosal expression of inflammatory cytokines IL-1α, IL-1β, IL-6, IL-8, MIP-1α and TNF promotes HPV elimination [17–19]. Our observations using an indirect HNSC cell and macrophage co-culture system suggest that HPV$^+$ HNSC cells induce macrophage M1 polarization through secreted factors. IL-6

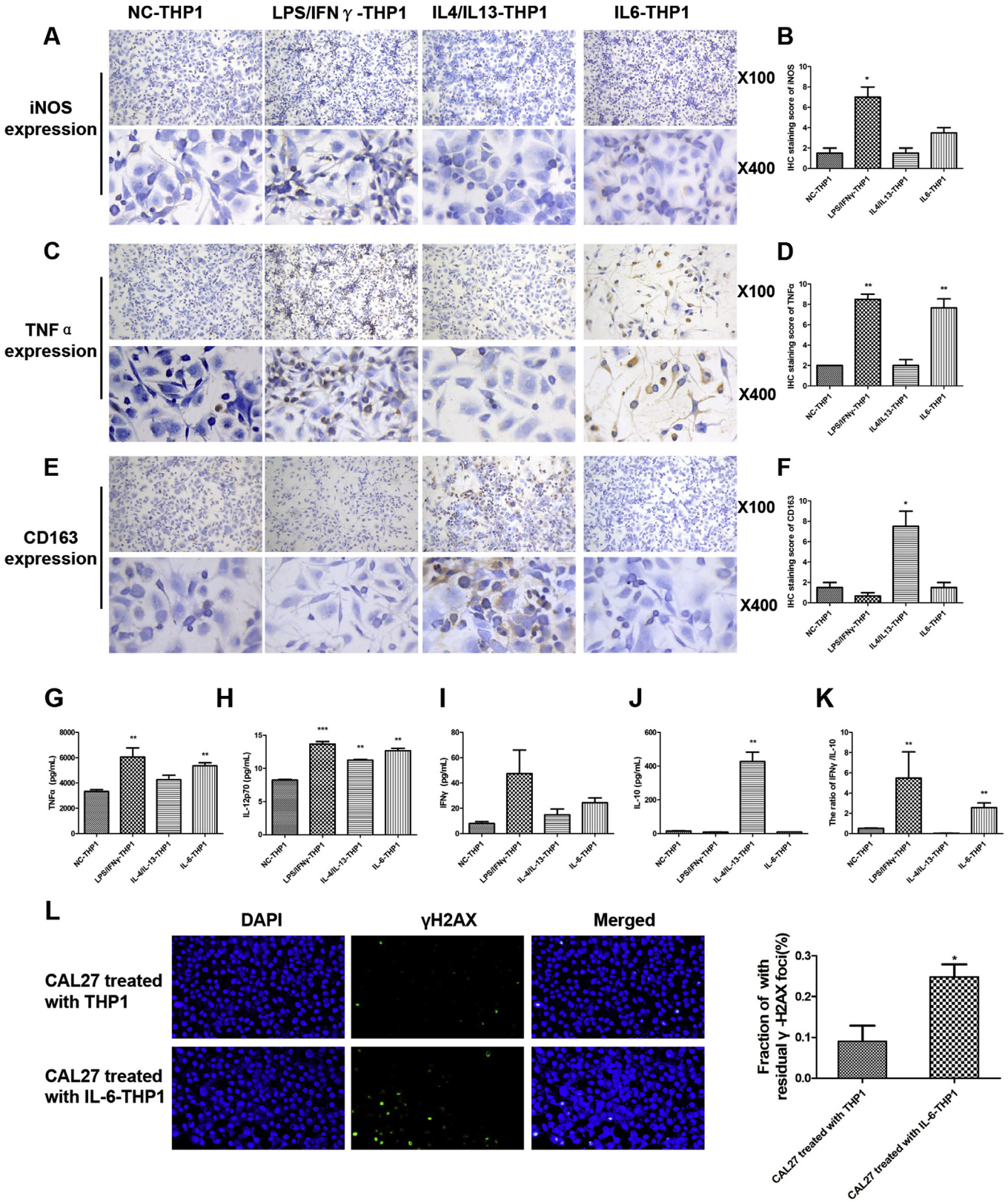

Fig. 6. Increased radiosensitivity through IL6-induced M1 macrophage polarization. (A) IHC analysis of iNOS expression in THP1-derived macrophages treated as indicated (NC, normal culture control)(magnification × 100 and × 400). **(B)** Quantitation of IHC iNOS expression data. **(C)** IHC analysis of TNFα expression in THP1-derived macrophages treated as indicated. **(D)** Quantitation of IHC TNFα expression data. **(E)** IHC analysis of CD163 expression in THP1-derived macrophages. **(F)** Quantitation of IHC CD163 expression data. **(G–K)** Multi-cytokine assay results. **(L)** Immunofluorescence detection of γ-H2AX foci 24 h after irradiation of CAL27 cells (magnification × 200). Quantitative analysis based on triplicate experiments. Data presented as mean ± SEM. $^{*}P < 0.05$,$^{**}P < 0.01$, $^{***}P < 0.001$.

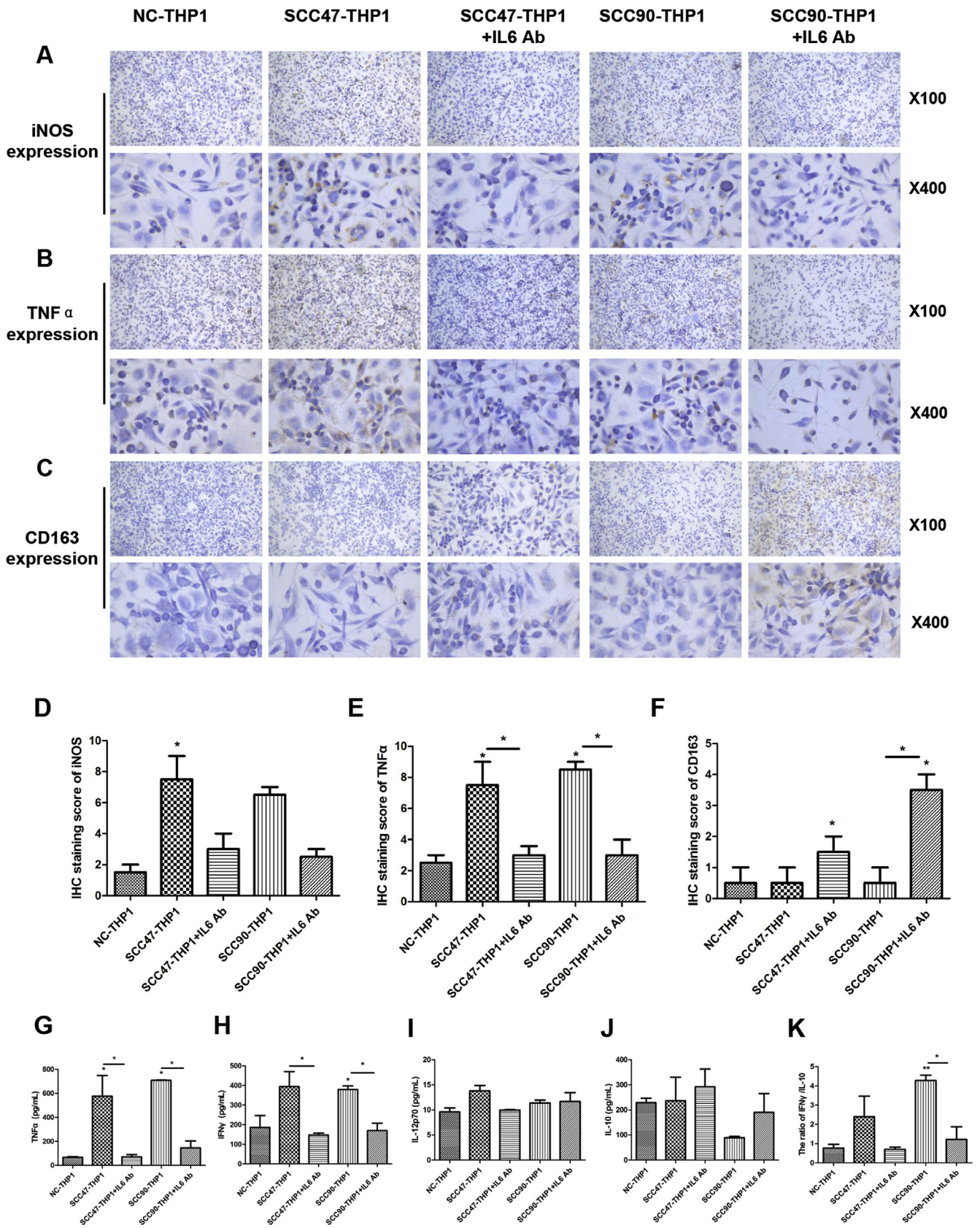

Fig. 7. IL-6 required for HPV associated M1 type macrophage polarization. (A) IHC analysis of iNOS expression in THP1 cells co-cultured with HNSC cells with and without addition of anti-IL6 antibody (IL6 Ab) (NC, normal culture control; SCC47 and SCC90, HPV^+ HNSC cell line co-culture)(magnification × 100 and × 400). **(B)** IHC analysis of TNFα expression in THP1 cells co-cultured with HNSC cells with and without addition of anti-IL6 antibody. **(C)** IHC analysis of CD163 expression in THP1 cells co-cultured with HNSC cells with and without addition of anti-IL6 antibody. **(D)** Quantitation of IHC iNOS expression data. **(E)** Quantitation of IHC TNFα expression data. **(F)** Quantitation of IHC CD163 expression data. **(G–K)** Multi-cytokine assay results. Quantitative analysis based on triplicate experiments. Data presented as mean ± SEM. $^*P < 0.05$,$^{**}P < 0.01$.

is involved in the progression of chronic inflammation to cancer, but studies do not show consistent roles of IL-6 in different cancers involving diverse signaling pathways [20]. IL-6 is well known as a promoter of lymphocyte activation, proliferation and survival during the immune response [21]. Since IL-6 is a classical marker representing M1 macrophage, there is controversial for the induction of M1/M2 macrophage polarization [22]. In some cases IL-6 could generate M2 macrophage partially. But the researchers found that IL-6 induced macrophage expressed high levels of CD86 (a M1 macrophage marker) and exhibited no obvious M2 phenotype function compared with IL-6 combined with hypoxia group [23]. The function of IL-6 on macrophage polarization was complicated since IL-6 could be affected by the local microenvironment. In the current study we showed significantly higher secretion of IL-6 by HPV^+ HNSC cells compared to HPV^- HNSC cells. Furthermore, transfection of HPV^- HNSC cells with full-length HPV and HPV16 E7 plasmids led to increased IL-6 secretion. Our findings are consistent with IL-6 involvement in HPV linked M1 polarization in the HNSC tissue microenvironment.

Programmed cell death protein-1 (PD-1) and its ligand, programmed death ligand 1 (PD-L1) mediate immune tolerance and promote the formation of an immunoprivileged site for tumor progression. Through the bioinformatic analyses of HNSC from TCGA, we indeed found that HPV^+ HNSC expressed higher level of PD-1 and PD-L1 (data not shown). One of the HNSC subtype which is depleted for both $CD8^+$ T cells and PD-1 expressing TAMs maybe particularly resistant to PD-1/PD-L1 checkpoint blockade immunotherapy [24]. And there exists positive regulation between M1 macrophages and $CD8^+$ T cells [25]. Anti-PD-L1 treatment can favorably remodel the macrophage compartment in responsive tumor models towards M1 phenotype [26]. They also suggest that directly targeting TAMs with reprogramming and depleting agents may further augment the breadth and depth of response to anti-PD-L1 treatment in HPV + HNSC microenvironment.

This study has elucidated a new mechanism to explain the increased radiosensitivity of HPV^+ HNSC. HPV stimulates IL-6 secretion that promotes polarization of macrophages to an M1 subtype. M1 macrophage prevalence is linked to an inflammatory tissue microenvironment that enhances radiation-induced DNA damage, an important factor in determining radiation treatment efficacy. While this mechanism involves complex immune networks that will require additional studies to define in detail, our results suggest that HPV status and M1 macrophage prevalence may be of value in the design of individualized treatment for HNSC patients.

Conflicts of interest

The authors declare that there are no conflicts of interest.

Acknowledgement

We thank Heilongjiang Provincial Key Laboratory of Infection and Immunity for providing the analytical platform used in this study. We thank the Key Laboratory of Pathogen Biology in Heilongjiang Provincial Education Institute for technical support. This study was supported by the Natural Science Foundation of China (81672670) and the Excellent Youth Foundation of Heilongjiang Province of China (JC2018023).

References

[1] D. Young, C.C. Xiao, B. Murphy, M. Moore, C. Fakhry, T.A. Day, Increase in head and neck cancer in younger patients due to human papillomavirus (HPV), Oral Oncol. 51 (2015) 727–730.

[2] K. Hoppe-Seyler, F. Bossler, J.A. Braun, A.L. Herrmann, F. Hoppe-Seyler, The HPV E6/E7 oncogenes: key factors for viral carcinogenesis and therapeutic targets, Trends Microbiol. 26 (2018) 158–168.

[3] N. Egawa, K. Egawa, H. Griffin, J. Doorbar, Human papillomaviruses; epithelial tropisms, and the development of neoplasia, Viruses 7 (2015) 3863–3890.

[4] H. Mirghani, F. Amen, Y. Tao, E. Deutsch, A. Levy, Increased radiosensitivity of HPV-positive head and neck cancers: Molecular basis and therapeutic perspectives, Cancer Treat Rev. 41 (2015) 844–852.

[5] G.D. Grass, E. Welsh, A.E. Berglund, F. Pettersson, J.J. Mulé, L.B. Harrison, S.A. Eschrich, J.F. Torres-Roca, Intrinsic immune landscapes between radiosensitive and radioresistant tumors, Int. J. Radiat. Oncol. Biol. Phys. 99 (2017) S23.

[6] A. Yuan, Y.J. Hsiao, H.Y. Chen, H.W. Chen, C.C. Ho, Y.Y. Chen, Y.C. Liu, T.H. Hong, S.L. Yu, J.J. Chen, P.C. Yang, Opposite effects of M1 and M2 macrophage subtypes on lung cancer progression, Sci. Rep. 5 (2015) 14273.

[7] M.M. Leblond, E.A. Peres, C. Helaine, A.N. Gerault, D. Moulin, C. Anfray, D. Divoux, E. Petit, M. Bernaudin, S. Valable, M2 macrophages are more resistant than M1 macrophages following radiation therapy in the context of glioblastoma, Oncotarget 8 (2017) 72597–72612.

[8] X. Chen, B. Yan, H. Lou, Z. Shen, F. Tong, A. Zhai, L. Wei, F. Zhang, Immunological network analysis in HPV associated head and neck squamous cancer and implications for disease prognosis, Mol. Immunol. 96 (2018) 28–36.

[9] J. Zhang, Y. Zhang, S. Liu, Q. Zhang, Y. Wang, L. Tong, X. Chen, Y. Ji, Q. Shang, B. Xu, M. Chu, L. Wei, Metadherin confers chemoresistance of cervical cancer cells by inducing autophagy and activating ERK/NF-kappaB pathway, Tumour Biol.: J. Int. Soc. Oncodevelopmental Biol. Med. 34 (2013) 2433–2440.

[10] H. Willers, L. Gheorghiu, Q. Liu, J.A. Efstathiou, L.J. Wirth, M. Krause, C. von Neubeck, DNA damage response assessments in human tumor samples provide functional biomarkers of radiosensitivity, Semin. Radiat. Oncol. 25 (2015) 237–250.

[11] A. Menegakis, C. von Neubeck, A. Yaromina, H. Thames, S. Hering, J. Hennenlotter, M. Scharpf, S. Noell, M. Krause, D. Zips, M. Baumann, gammaH2AX assay in ex vivo irradiated tumour specimens: a novel method to determine tumour radiation sensitivity in patient-derived material, Radiother. Oncol.: J. Eur. Soc. Therapeut. Radiol. Oncol. 116 (2015) 473–479.

[12] P.J. Murray, J.E. Allen, S.K. Biswas, E.A. Fisher, D.W. Gilroy, S. Goerdt, S. Gordon, J.A. Hamilton, L.B. Ivashkiv, T. Lawrence, M. Locati, A. Mantovani, F.O. Martinez, J.L. Mege, D.M. Mosser, G. Natoli, J.P. Saeij, J.L. Schultze, K.A. Shirey, A. Sica, J. Suttles, I. Udalova, J.A. van Ginderachter, S.N. Vogel, T.A. Wynn, Macrophage activation and polarization: nomenclature and experimental guidelines, Immunity 41 (2014) 14–20.

[13] A.P. Sowjanya, M. Rao, H. Vedantham, B. Kalpana, U.R. Poli, M.A. Marks, M. Sujatha, Correlation of plasma nitrite/nitrate levels and inducible nitric oxide gene expression among women with cervical abnormalities and cancer, Nitric Oxide : Biol. Chem. 52 (2016) 21–28.

[14] M. Polz-Dacewicz, M. Strycharz-Dudziak, J. Dworzanski, A. Stec, J. Kocot, Salivary and serum IL-10, TNF-alpha, TGF-beta, VEGF levels in oropharyngeal squamous cell carcinoma and correlation with HPV and EBV infections, Infect. Agents Cancer 11 (2016) 45.

[15] L. Gao, F.Q. Wang, H.M. Li, J.G. Yang, J.G. Ren, K.F. He, B. Liu, W. Zhang, Y.F. Zhao, CCL2/EGF positive feedback loop between cancer cells and macrophages promotes cell migration and invasion in head and neck squamous cell carcinoma, Oncotarget 7 (2016) 87037–87051.

[16] S.A. Lorimore, P.J. Coates, E.G. Wright, Radiation-induced genomic instability and bystander effects: inter-related nontargeted effects of exposure to ionizing radiation, Oncogene 22 (2003) 7058–7069.

[17] C. Colin-Ferreyra Mdel, H. Mendieta-Zeron, S. Romero-Figueroa Mdel, M. Martinez-Madrigal, S. Martinez-Perez, M.V. Dominguez-Garcia, [Expression of gamma interferon during HPV and Chlamydia trachomatis infection in cervical samples], Enfermedades Infecc. Microbiol. Clínica 33 (2015) 105–109.

[18] I. Ushach, A. Zlotnik, Biological role of granulocyte macrophage colony-stimulating factor (GM-CSF) and macrophage colony-stimulating factor (M-CSF) on cells of the myeloid lineage, J. Leukoc. Biol. 100 (2016) 481–489.

[19] C.T. Allen, P.E. Clavijo, C. Van Waes, Z. Chen, Anti-tumor immunity in head and neck cancer: understanding the evidence, how tumors escape and immunotherapeutic approaches, Cancers 7 (2015) 2397–2414.

[20] K. Heikkila, S. Ebrahim, D.A. Lawlor, Systematic review of the association between circulating interleukin-6 (IL-6) and cancer, Eur. J. Cancer 44 (2008) 937–945 Oxford, England : 1990.

[21] H.H. Aarstad, O.K. Vintermyr, E. Ulvestad, K. Kross, J.H. Heimdal, H.J. Aarstad, In vitro-stimulated IL-6 monocyte secretion and in vivo peripheral blood T lymphocyte activation uniquely predicted 15-year survival in patients with head and neck squamous cell carcinoma, PLoS One 10 (2015) e0129724.

[22] H. Qin, A.T. Holdbrooks, Y. Liu, S.L. Reynolds, L.L. Yanagisawa, E.N. Benveniste, SOCS3 deficiency promotes M1 macrophage polarization and inflammation, J. Immunol. 189 (2012) 3439–3448 Baltimore, Md. : 1950.

[23] J. Zhang, J. Cao, S. Ma, R. Dong, W. Meng, M. Ying, Q. Weng, Z. Chen, J. Ma, Q. Fang, Q. He, B. Yang, Tumor hypoxia enhances Non-Small Cell Lung Cancer metastasis by selectively promoting macrophage M2 polarization through the activation of ERK signaling, Oncotarget 5 (2014) 9664–9677.

[24] K. Brennan, J.H. Shin, J.K. Tay, M. Prunello, A.J. Gentles, NSD1 inactivation defines an immune cold, DNA hypomethylated subtype in squamous cell carcinoma, 7 (2017) 17064.

[25] X. Chen, B. Yan, H. Lou, Z. Shen, F. Tong, A. Zhai, L. Wei, F. Zhang, Immunological network analysis in HPV associated head and neck squamous cancer and implications for disease prognosis, Mol. Immunol. 96 (2018) 28–36.

[26] H. Xiong, S. Mittman, R. Rodriguez, M. Moskalenko, P. Pacheco-Sanchez, Y. Yang, D. Nickles, R. Cubas, Anti-PD-L1 treatment results in functional remodeling of the macrophage compartment, Cancer Res. 79 (2019) 1493–1506.